Journal of Inflammation Research

Dovepress
open access to scientific and medical research

Open Access Full Text Article

ORIGINAL RESEARCH

CORM-3 Inhibits the Inflammatory Response of Human Periodontal Ligament Fibroblasts Stimulated by LPS and High Glucose

Haoyang Tian[1,*], Hui Chen[2,*], Xiaochun Yin[2], Meiyi Lv[3], Lingling Wei[1], Yuna Zhang[4], Shuhan Jia[5], Jingyuan Li[1], Hui Song[1]

[1]School and Hospital of Stomatology, Cheeloo College of Medicine, Shandong University & Shandong Key Laboratory of Oral Tissue Regeneration & Shandong Engineering Laboratory for Dental Materials and Oral Tissue Regeneration & Shandong Provincial Clinical Research Center for Oral Diseases, Jinan, People's Republic of China; [2]Department of Endodontics, Jinan Stomatological Hospital, Jinan, People's Republic of China; [3]Department of Pediatric Dentistry, Jinan Stomatological Hospital, Jinan, People's Republic of China; [4]Department of Stomatology, The First Affiliated Hospital of Guangxi Medical University, Nanning, People's Republic of China; [5]Department of Stomatology, Yancheng NO. 1 People's Hospital, Yancheng, People's Republic of China

*These authors contributed equally to this work

Correspondence: Hui Song; Jingyuan Li, School and Hospital of Stomatology, Cheeloo College of Medicine, Shandong University & Shandong Key Laboratory of Oral Tissue Regeneration & Shandong Engineering Laboratory for Dental Materials and Oral Tissue Regeneration & Shandong Provincial Clinical Research Center for Oral Diseases, No. 44-1 Wenhua Road West, Jinan, Shandong, 250012, People's Republic of China, Tel +86-531-88382912, Fax +86-531-88382923, Email songhui@sdu.edu.cn; jingyuan_31@163.com

Introduction: Diabetes has been recognized as an independent risk factor for periodontitis. Increasing evidences indicate that hyperglycemia aggravates inflammatory response of human periodontal ligament cells (hPDLCs). Carbon monoxide-releasing molecule-3 (CORM-3) is a water-soluble compound that can release carbon monoxide (CO) in a controllable manner. CORM-3 has been shown the anti-inflammatory effect in different cell lineages.

Methods: We stimulated periodontal ligament cells with LPS and high glucose. The expression of inflammatory cytokine was detected by ELISA. RT-qPCR, Western blot and immunofluorescence were used to detect the expression of TLR2, TLR4, RAGE and the activation of NF-κB pathway. We performed silencing and overexpression treatment of RAGE targeting the role of RAGE. We performed the immunostaining of paraffin sections of the periodontitis model in diabetes rats.

Results: The results showed that CORM-3 significantly inhibited the expression of inflammatory cytokine in hPDLCs stimulated with LPS and high glucose. CORM-3 also inhibited LPS and high glucose-induced expression of RAGE/NF-κB pathway and TLR2/TLR4/NF-κB pathway. Silence of RAGE resulted in significantly decreased expression of proteins above. Overexpression of RAGE significantly enhanced the expression of these factors. CORM-3 abrogated the effect of RAGE partially. In animal model, CORM-3 suppressed the inflammatory response of periodontal tissues in experimental periodontitis of diabetic rats.

Discussion: Our research proved CORM-3 reduced the inflammatory response via RAGE/NF-κB pathway and TLR2/TLR4/NF-κB pathway in the process of high glucose exacerbated periodontitis. These findings demonstrated the role of RAGE in the process of high glucose exacerbated periodontitis and suggested that CORM3 be a potential therapeutic strategy for the treatment of diabetes patients with periodontitis.

Keywords: carbon monoxide-releasing molecules, periodontitis, diabetes, receptor for advanced glycation end products, lipopolysaccharide

Introduction

Periodontitis, triggered by the pathogenic bacteria residing in the subgingival plaque, features a chronic inflammation in periodontal tissues, leading to connective tissue destruction, alveolar bone resorption and tooth loss eventually.[1] In response to bacterial and its products, multiple immunocytes including monocyte/macrophages and lymphocytes are recruited from peripheral blood to local periodontal tissue, in which they release a series of inflammatory cytokines

Received: 23 January 2024
Accepted: 18 June 2024
Published: 22 July 2024

Graphical Abstract

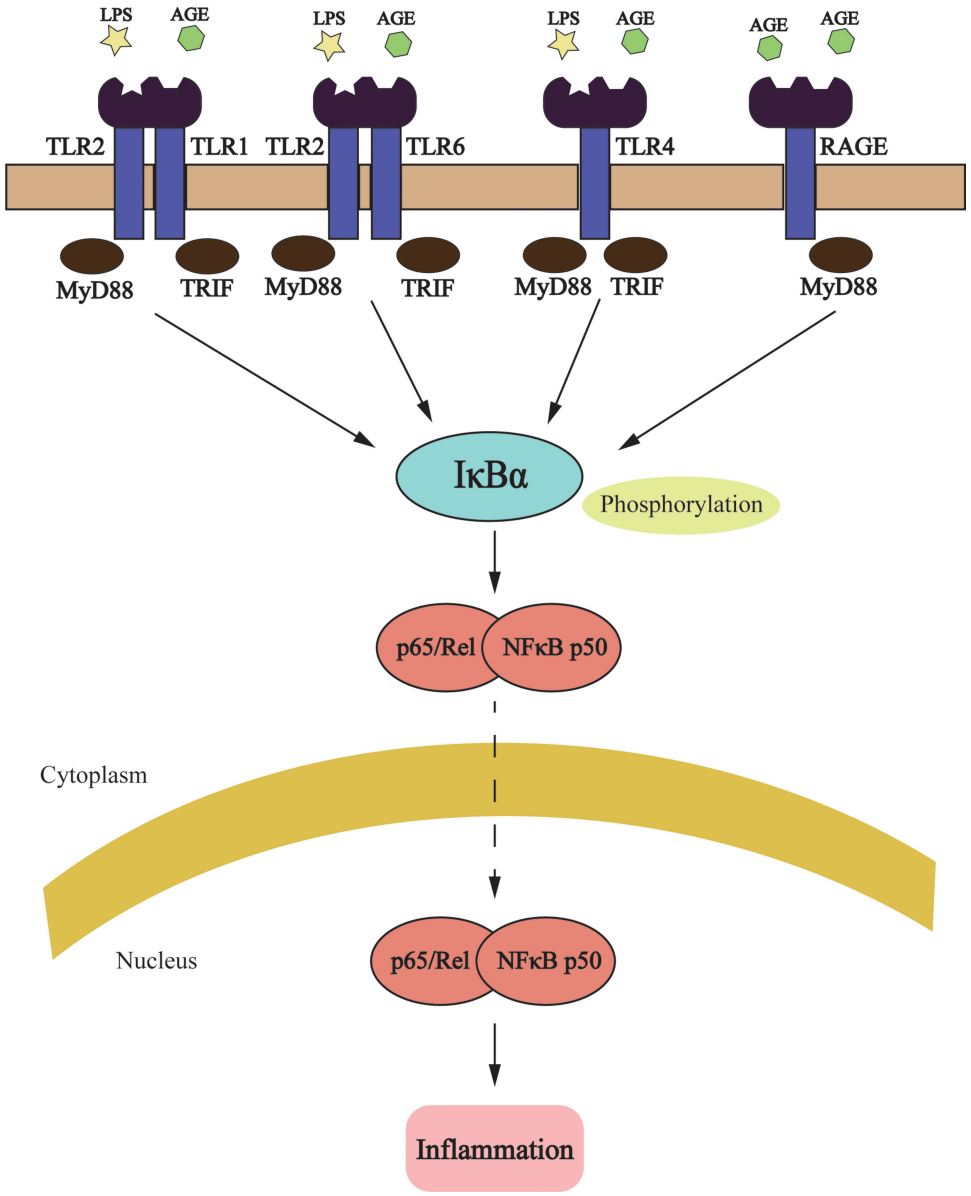

resulting in periodontal tissue destruction.[2] A number of studies have shown a bi-directional relationship between periodontitis and diabetes. There is a significant rise in incidence of periodontitis for diabetic patients, on the other hand, the relative risk of developing diabetes is also significantly increased for patients with periodontitis.[3,4] Diabetes may lead to morphological and epigenetic changes in the periodontium, altering the defense status of the tissue and increasing the susceptibility of the host to periodontal disease.[5] Studies showed that patients with type 2 diabetes and periodontitis who received nonsurgical periodontal therapy had significantly lower level of HbA1c and fasting plasma glucose than those with no periodontal treatment. Periodontal therapy directly improves periodontal health and reduces HbA1c level, thereby reducing the likelihood of inflammation-induced prediabetes in patients with chronic periodontitis.[6–8] Both type 1 and type 2 diabetes induce the increased expression of inflammatory cytokines in human periodontium.[9] However, the mechanism by which periodontitis is aggravated by diabetes remains unclear.

The possible association mechanism between diabetes and periodontal disease includes the release of advanced glycation end (AGE) products due to hyperglycemia, and a series of common predisposing factors of genetic, microbial and lifestyle properties.[10] AGE has been determined as an independent risk indicator of severe periodontitis.[11] AGEs mainly bind to specific receptor for advanced glycation end products (RAGE). RAGE, a multi-ligand transmembrane receptor belonging to the immunoglobulin superfamily, has been reported to be able to regulate innate immunity.[12] As a pattern recognition receptor (PRR), RAGE has a high affinity for AGEs and mediates the effect through receptor-dependent pathway.

RAGE has a variety of ligands, such as HMGB1, AGEs, S100/calcium granule protein family, and Mac-1β Lamellar fibrils. Lipopolysaccharide (LPS) mainly combine with the V domain of RAGE. More and more evidences show that the interaction of AGEs and the receptor (RAGE) leads to oxidative stress, inflammatory response, formation of blood clots and calcification in arterial walls. In this way, AGE products are involved in the aging of blood vessels and numerous damages.[13,14] After ligand binding, RAGE activates multiple intracellular signal pathways, involving NFκB, mitogen-activated protein kinase (MAPK), guanine nucleotide triphosphatase (GTPases), and phosphocreatine 3-kinase (PI3-K)/Akt, etc, initiating the transcription of a cluster of pro-inflammatory genes including adhesion molecules (ICAM-1, VCAM-1), cytokines (IL-1, IL-6, TNF-α), and enzymes related to oxidative stress. RAGE is expressed in a variety of cell types, including endothelial cells, vascular smooth muscle, cancer cells, monocytes/macrophages, granulocytes and adipocytes. It is reported that the expression of RAGE is up-regulated in diabetes, atherosclerosis, rheumatoid arthritis, Alzheimer's disease (AD), cardiovascular disease (CVD) and immune/inflammatory diseases. Increased expression of RAGE has also been proved to be related to the development and progress of cancer.[15]

AGEs bind to the receptor RAGE on the cell surface and up regulate its expression, which is aggravated by the positive feedback loop in diabetes.[16] Due to the co-localization of AGEs and RAGE, the increased accumulation of AGEs up-regulates the expression of RAGE through the activation of NFκB-p65 mainly.[17] In addition to activating NFκB and mediating inflammation, RAGE also regulates the expression of TNF-α and VEGF, and modulates the oxidative stress and endothelial dysfunction in type 2 diabetes.[18] It has been reported that anti-RAGE antibody improves diabetes retinopathy in Wistar rats through hypoglycemic and anti-inflammatory effect.[19]

Periodontal ligament fibroblasts (PDLCs) account for the majority of the periodontal membrane. These fibroblasts fulfill abundant functions including the maintenance of tissue homeostasis and the establishment of a collagenous extracellular matrix by secreting structural proteins, as well as the regulation in the defensive responses of the innate immune system.[20] Under high-glucose conditions, PDLCs exhibit inhibited proliferation and differentiation potentials, and increased apoptosis, which further disrupts the homeostasis and decreases the regenerative ability of periodontal tissues.[21,22]

Carbon monoxide (CO) is a colorless and odorless gaseous molecule. It is an endogenous product of heme degradation by heme oxygenase 1 (HO-1).[23] CO has long been considered as the poisonous agent since it disrupts oxygen delivery to the tissue due to its high affinity for hemoglobin.[24] However, accumulating evidences suggest that CO is able to suppress inflammation,[25] modulate vasoactivity,[26] attenuate ischemia-reperfusion injury,[27,28] and destroy the pathogenic microorganisms.[29,30] Interestingly, as a product of HO-1, CO, in turn, can induce a high expression of HO-1.[31] Carbon monoxide-releasing molecules (CORMs) are a group of transition metal carbonyl-based compounds able to deliver controlled quantities of exogenous CO without elevating carboxyhemoglobin (COHb) to toxic levels.[32,33] As a member of CORMs family, CORM-3 [tricarbonylchloro (glyconato) ruthenium (II)] is fully water-soluble and can rapidly release CO in a controllable manner[34] when dissolved in physiological solutions, which makes it a potential therapeutic strategy in the treatment of the disease. CORM-2 suppresses TXNIP/NLRP3 inflammasome pathway and protects against LPS-induced lung injury. From this, it can be seen that carbon monoxide may have anti-inflammatory effects on periodontitis.[35]

We previously reported that CORM-3 promotes the osteogenic differentiation of mesenchymal stems cells and suppresses inflammatory cytokines release in lipopolysaccharide-stimulated human periodontal ligament cells, suggesting the potential of CORM-3 in the treatment of inflammatory periodontal disease.[36,37] However, whether CORM-3 has a beneficial effect on periodontitis concomitant with diabetes remains unknown. In this study, we used LPS and high glucose costimulated human PDLCs as an in vitro model to mimic the cellular environment of periodontitis with diabetes mellitus. We investigated the effect of CORM-3 on the inflammatory response in cells stimulated with LPS and high glucose, and explored the possible mechanism underlying the regulatory effect of CORM-3. We also used diabetic rats

with experimental periodontitis as an in vivo model to study the effect of CORM-3 on inflammatory responses in periodontal tissues.

Materials and Methods

Cell Isolation and Culture

The study was approved by the ethics committee of the Stomatological Hospital of Shandong University (Jinan, China) (approval number: 20220117). Periodontal ligamental tissues were separated from the premolars or third molars from 14 patients (6 males and 8 females) aged between 16 and 24 years for orthodontic treatment between August 2022 and September 2023 in Stomatological Hospital of Shandong University. All patients were provided informed written consent to participate in this study. The tissues were scraped and then cut into small pieces, and cultured in 25 cm^2 culture bottles (Corning Inc., NY, USA) supplemented with 1% 100x penicillin-streptomycin solution (HyClone, California, USA), 20% heat-inactivated fetal bovine serum (FBS; Kibbutz Beit-Haemek, Israel) and 79% Dulbecco's modified Eagle's medium (DMEM; Biological Industries, Kibbutz Beit-Haemek, Israel) in humidified air with 5% CO_2 at 37°C. The hPDLCs were collected and sub-cultured when they reached 80% confluence with the medium changed every 2 d. Cells between the 3rd and 5th passages were used in the experiments.

Immunocytochemistry

Cells were fixed with precooled Paraformaldehyde for 30 min, incubated for 10 min with PBS containing either 0.1% Triton X-100, incubate with 5% BSA for 60 min to block unspecific binding of the antibodies and then incubated with vimentin (1:200; Abcam, Cambridge, UK), cytokeratin 17 antibodies (1:200; Proteintech, IL, USA), and rabbit anti-human p65 (1:1000; Cell Signaling Technology, USA) antibody. After being washed with PBS for 3 times, the cells were incubated with the FITC secondary antibody goat anti-rabbit IgG(H+L) (1:200; Proteintech, Chicago, USA) at room temperature for 1 hour. Then, the cells were redyed with 4, 6-diamino-2-phenylindole (DAPI) (Solarbio, Beijing, China). Images were taken with a Zeiss LSM 880 laser-scanning microscope and analyzed using the LSM Software ZEN 2009 (Carl Zeiss, Oberkochen, Germany).

Cell Treatment

Sub-cultured hPDLCs were divided into 4 groups as follows: Control group, in which the cells were cultured in control medium (cell growing medium containing 5.6 mM D-glucose); LPS treatment group, in which the cells were incubated in control medium containing 10 μg/mL LPS (Sigma-Aldrich, Missouri, USA); LPS + high glucose co-treatment group, in which the cells were cotreated with high glucose medium containing 10 μg/mL LPS and 45 mM D-glucose (Sigma-Aldrich, Missouri, USA); LPS + high glucose + CORM-3 group, in which the cells were pretreated with CORM-3 (400 μM; Sigma-Aldrich, Missouri, USA) for 24 h prior to incubation in high glucose medium containing 10 μg/mL LPS and 45 mM D-glucose.

ELISA Assay

For measurement of cytokine releasing, hPDLCs were incubated in 24-well plates for 48 h. The supernatant was collected and stored at −20°C for use. Cytokine concentration of IL-1β, IL-6, IL-8 and IL-10 in the supernatant was determined by sandwich ELISA (R&D systems, Minnesota, USA) using MaxiSorp plates (Nunck, Rochild, Denmark) according to manufacturer's instructions.

RT-qPCR

Total RNA was extracted using TRIzol (Invitrogen, CA, USA) according to the manufacturer's instructions. The purity and concentration of the extracted RNA were analyzed using the NanoDrop (Thermo Fisher Scientific, Waltham, MA, USA). Complementary DNA (cDNA) was synthesized from 1 μg total RNA using an Evo M-MLV Reverse transcription Kit (Accurate Biology, Changsha, Hunan, China) following the manufacturer's protocol. RT-qPCR reactions were performed in a Light Cycler II Real-time PCR system (Roche, Basel, Switzerland) using the SYBR Premix Ex Taq

(Roche, Basel, Switzerland) to detect mRNA levels of related molecules. Thermocycling conditions consisted of 95°C for 30s, followed by 45 cycles of denaturation at 95°C for 5 s and annealing at 60°C for 30s. The primers used (Accurate Biology, Changsha, Hunan, China) were as follows:

homo-TLR2: Forward 5'-ACCGTTTCCATGGCCTGTG-3'
Reverse 5'-GATGTTCCTGCTGGGAGCTTTC-3'
homo-TLR4: Forward 5'-TTATCACGGAGGTGGTTCCTA-3'
Reverse 5'-TCAGGTCCAGGTTCTTGGTTG-3'
homo-RAGE: Forward 5'-GACTCTTAGCTGGCACTTGGAT-3'
Reverse 5'-GTCTCCTGGTCTGTTCCTTCAC-3'
homo-MyD88: Forward 5'-CTTGGTTCTGGACTCGCCTTG-3'
Reverse 5'-AGCACAGATTCCTCCTACAACGA-3'
homo-p65: Forward 5'-GACGCATTGCTGTGCCTTC-3'
Reverse 5'-TTGATGGTGCTCAGGGATGAC-3'
homo-p50: Forward 5'-AGCCTCCAGCCCAGTGAAGA-3'
Reverse 5'-CACCACTGGTCAGAGACTCGGTAA-3'
homo-IκBα: Forward 5'-GAAGTGATCCGCCAGGTGAA-3'
Reverse 5'-CTCACAGGCAAGGTGTAGGG-3'
homo-GAPDH: Forward 5'-GCACCGTCAAGGCTGAGAAC-3'
Reverse 5'-TGGTGAAGACGCCAGTGGA-3'

Each sample was tested in triplicate and gene expression levels were analyzed using LightCycler 480 software 1.5 (Roche Diagnostics). Data were calculated using the $2^{-\Delta\Delta Ct}$ method, and presented as fold-change relative to the control.

Western Blot

The hPDLCs were lysed using radioimmunoprecipitation assay lysis buffer (Beyotime Institute of Biotechnology, Shanghai, China) containing protease inhibitor (1:100) and stored at −80°C for later use. The protein concentrations were determined by measuring the absorbance at 562 nm using a BCA protein assay solution (Beyotime Institute of Biotechnology, Shanghai, China). Protein samples were firstly boiled at 100°C for 5 min with loading buffer (1:4) added, and then further separated on 10% SDS-polyacrylamide gel electrophoresis gels in migration buffer (Solarbio Science & Technology, Beijing, China), and transferred onto polyvinylidene difluoride membranes (PVDF; Amersham Pharmacia Biotech, Piscataway, NJ, USA). Membranes were blocked using 5% skimmed milk for 1 hour and further incubated with primary antibodies for 16 hours at 4°C. The antibodies used were rabbit anti-human TLR2 (1:1000; Abcam, UK), rabbit anti-human TLR4 (1:1000; Abcam, UK), rabbit anti-human p65 (1:1000; Cell Signaling Technology, USA), rabbit anti-human P-p65 (1:1000; Cell Signaling Technology, USA), rabbit anti-human p50 (1:1000; Absin, China), rabbit anti-human P-p50 (1:1000; Absin, China), rabbit anti-human IκBα (1:1000; Cell Signaling Technology, USA), rabbit anti-human P-IκBα (1:1000; Cell Signaling Technology, USA), rabbit anti-human RAGE (1:1000; Abcam, UK), and HRP-GAPDH (1:10000; Proteintech, USA). After washing three times with 1×TBST, the membranes were incubated with secondary antibodies for 1 hour at 20°C. The secondary antibodies used were goat anti-mouse immunoglobulin G (IgG)-horseradish peroxidase (HRP; 1:1000; Proteintech, USA), or goat anti-rabbit IgG-HRP (1:1000; Proteintech, USA). Immunoreactive bands were revealed by chemiluminescence (Millipore, Billerica, MA, USA) and a ChemiScope Western Blot Imaging System (Clinx Science Instruments, Shanghai, China). Protein band densities on scanned films were analyzed using the Image J software. GAPDH was used as a loading control.

Silent Expression and Overexpression of RAGE

RAGE siRNA, RAGE siRNA NC, RAGE overexpression vector and empty vector were designed and constructed by Jinan Boshang biological Inc. The design sequences displayed in the supporting information (Figure S1).

The hPDLCs of passage 3–5 in good growth condition were seeded into 6-well plates with 4×10^5 cells per well. 6 μL lipo2000 transfection reagent (Invitrogen, California, USA) was added to 150 μL opti-MEM (Gibco, California, USA), 3 μg RAGE siRNA/overexpression vector and 3 μg siRNA NC/empty vector were added to another 150 μL opti-MEM, respectively. The RNA containing solution was dropwise added to the solution containing transfection reagent in

a volume ratio of 1:1. After 5 min incubation at room temperature, 250 μL mixed solution was added to one well and cultured in incubator. After 6 h, fresh culture solution was replaced.

Transfection efficiency was tested by RT-qPCR and Western blot. Sub-cultured hPDLCs were divided into 5 groups as follows: Control group, in which the cells were incubated with 10 μg/mL LPS and 45 mM D-glucose (Sigma-Aldrich); siRNA NC/empty vector group, in which the cells were transfected with siRNA NC/empty vector and incubated with LPS and high glucose; siRNA NC/empty vector + CORM group, in which the cells were transfected with siRNA NC/empty vector and incubated with LPS, high glucose and 400 μM CORM-3; RAGE siRNA/overexpression vector group, in which the cells were transfected with RAGE siRNA/overexpression vector and incubated with LPS and high glucose; RAGE siRNA/overexpression vector + CORM group, in which the cells were transfected with RAGE siRNA/overexpression vector and incubated with LPS, high glucose and CORM-3.

Establishment of Animal Models

The animal experimental protocol was approved by the ethics committee of Stomatological Hospital of Shandong University (approval number: 20210610). Twenty 6-week-old male Wistar rats (Weitonglihua, China) weighing around 180g were purchased for in vivo experiments. All experimental animals were kept in the SPF level experimental animal center, ensuring a comfortable living environment such as drinking water, diet, and temperature for the experimental animals. The animals were divided into 4 groups as follows: Control group, healthy rats without any treatment; Chronic periodontitis (CP) group, experimental periodontitis rat model; Diabetes mellitus (DM) + CP group, experimental periodontitis model in diabetes rats; CORM + DM + CP group, experimental periodontitis model in diabetes rats, CORM-3 solution (10 mg/kg) was injected intraperitoneally every other day.

Establishment of diabetes rat model: 2% STZ solution was prepared with 0.1 mol/L sodium citrate buffer (pH 4.5). Experimental diabetes rats were fed with high sugar and high fat diet for 2 weeks. They were injected with 2% STZ solution intraperitoneally at a dose of 30 mg/kg every other day with three times in total. The blood glucose of tail vein was measured 3 days after the last injection. The rats with blood glucose ≥16.65 mmol/L were determined as experimental diabetes rats. If the blood glucose is not up to the standard, STZ solution was injected with the same dose and frequency as before until the blood glucose reached the standard.

Establishment of the periodontitis model in diabetes rats: The neck of the right maxillary second molar of the diabetes rat was wrapped with 4–0 surgical suture, and the knot was tied on the buccal side. The suture was put into the gingival sulcus, and 20 μL *P.g* solution was injected into the buccal-lingual gingival sulcus of the right maxillary second molar. The clinical criteria for the success of experimental periodontitis rat model include gingival inflammation, loss of attachment, alveolar bone resorption, and increased probing depth.

Immunohistochemical Staining

Two weeks after the establishment of periodontitis, the maxillary tissues were isolated. After the heart perfusion, the right maxillary tissues were placed in paraformaldehyde fixed solution for 24 hours, and then placed in 10% EDTA decalcification solution. The sample was then dehydrated, embedded in paraffin, and sectioned on a microtome along the buccal-lingual direction. Labeled streptavidin biotinylated antibody method was used for the detection of the expression of RAGE. Rabbit monoclonal antibody against RAGE (1:500; Abcam, UK) was used for the primary reaction. For the subsequent reaction, we used labeled streptavidin biotin kit (ZSGB-BIO, Beijing, China). For the expression of NF-κB p65, samples were incubated with rabbit anti-human p65 (1:1000; Cell Signaling Technology, USA) at 4°C overnight. After being washed with PBS for 3 times, the cells were incubated with the FITC secondary antibody goat anti-rabbit IgG(H+L) (1:200; Proteintech, Chicago, USA) at room temperature for 1 hour. Then, the cells were redyed with 4,6-diamino-2-phenylindole (DAPI) (Solarbio, Beijing, China). Images were taken with a Zeiss LSM 880 laser-scanning microscope and analyzed using the LSM Software ZEN 2009 (Carl Zeiss, Oberkochen, Germany).

Statistical Analysis

Data are expressed as means ± standard deviation. All experiments were replicated at least three times. Data analyses and the significance of different groups were assessed using GraphPad Prism 6 software (GraphPad, CA, USA). Statistical significance was determined using one-way ANOVA followed by Tukey's multiple comparison test and p values of less than 0.05 were considered significant.

Results

Identification of hPDLCs

The expression of Vimentin and Cytokeratin 17 is shown in Figure 1A. The positive expression of Vimentin and the negative expression of Cytokeratin 17 demonstrated the typical characteristics of mesenchymal derived periodontal ligament cells.

CORM-3 Reduces LPS-Induced Release of Inflammatory Cytokines from hPDLCs in the Presence of High Glucose

Firstly, we screened the concentration of LPS and conducted CCK-8 and ELISA of IL1β. We found that LPS had no effect on the proliferation of hPDLC within a concentration range of no more than 10 μg/mL, while concentrations greater than 10 μg/mL had a significant toxic effect on hPDLC (Figure S2A). Meanwhile, there was a significant promotion of IL1β expression and release within a concentration range not exceeding 10 μg/mL, with 10 μg/mL having the most significant pro-inflammatory effect (Figure S2B). Our previous study indicated that 400 μM CORM-3 was capable of suppressing the expression of LPS-induced inflammatory cytokines without cytotoxicity to cells.[34] Based on the pre-experimental Results and the results of CCK8 (Figure S3), 400 μM was selected as the working concentration of CORM-3 for the following experiments. At the same time, we also selected the pre-treatment time for CORM-3 and found that it can reduce the release of inflammatory factors within 12 hours, reaching its lowest point at 24 hours. With the extension of time, there was no significant difference in the release of inflammatory factors (Figure S4). To determine of effects of CORM-3 on the inflammatory response of hPDLCs induced by LPS and high glucose, the expression of IL-1β, IL-6, IL-8 and IL-10 in cell supernatant was examined. As shown in Figure 1B–D, the protein levels of IL-1β, IL-6 and IL-8 secreted by hPDLCs were significantly increased with LPS stimulation. However, as an anti-inflammatory cytokine, the expression of IL-10 was significantly down-regulated, as shown in Figure 1E. Co-treatment of high glucose further enhanced the release of IL-1β, IL-6, IL-8 and inhibited the release of IL-10, compared with LPS treatment alone. With CORM-3 pretreatment, the increased expression levels of IL-1β, IL-6, IL-8 induced by LPS and high-glucose were partially abrogated, and a retrieve of IL-10 expression was also observed (Figure 1B–E). These results revealed that CORM-3 inhibited the enhanced inflammatory response of hPDLCs induced by LPS and high glucose.

CORM-3 Reduces LPS-Induced TLR2 and TLR4 Expression in hPDLCs in the Presence of High Glucose

Toll-like receptors play a crucial role in pathogen recognition and immunoresponse activation by delivering signals to the immune cells. Here, we tested the TLR2 and TLR4 expression in hPDLCs in response to LPS in the presence or absence of high glucose. The results showed that both the mRNA and protein expression of TLR2 in hPDLCs stimulated with LPS were significantly increased as compared with that in control group (Figure 2A and C), and the similar change trend was also observed for TLR4 (Figure 2B and D). Combined application of high glucose with LPS significantly enhanced TLR2 and TLR4 expression induced by LPS. Pretreatment with CORM-3 significantly inhibited the expression of TLR2 and TLR4 induced by cotreatment of LPS and high-glucose (Figure 2A–D), which indicated that TLRs expression might be involved in the regulatory effect of CORM-3 on LPS and high glucose-induced inflammatory response.

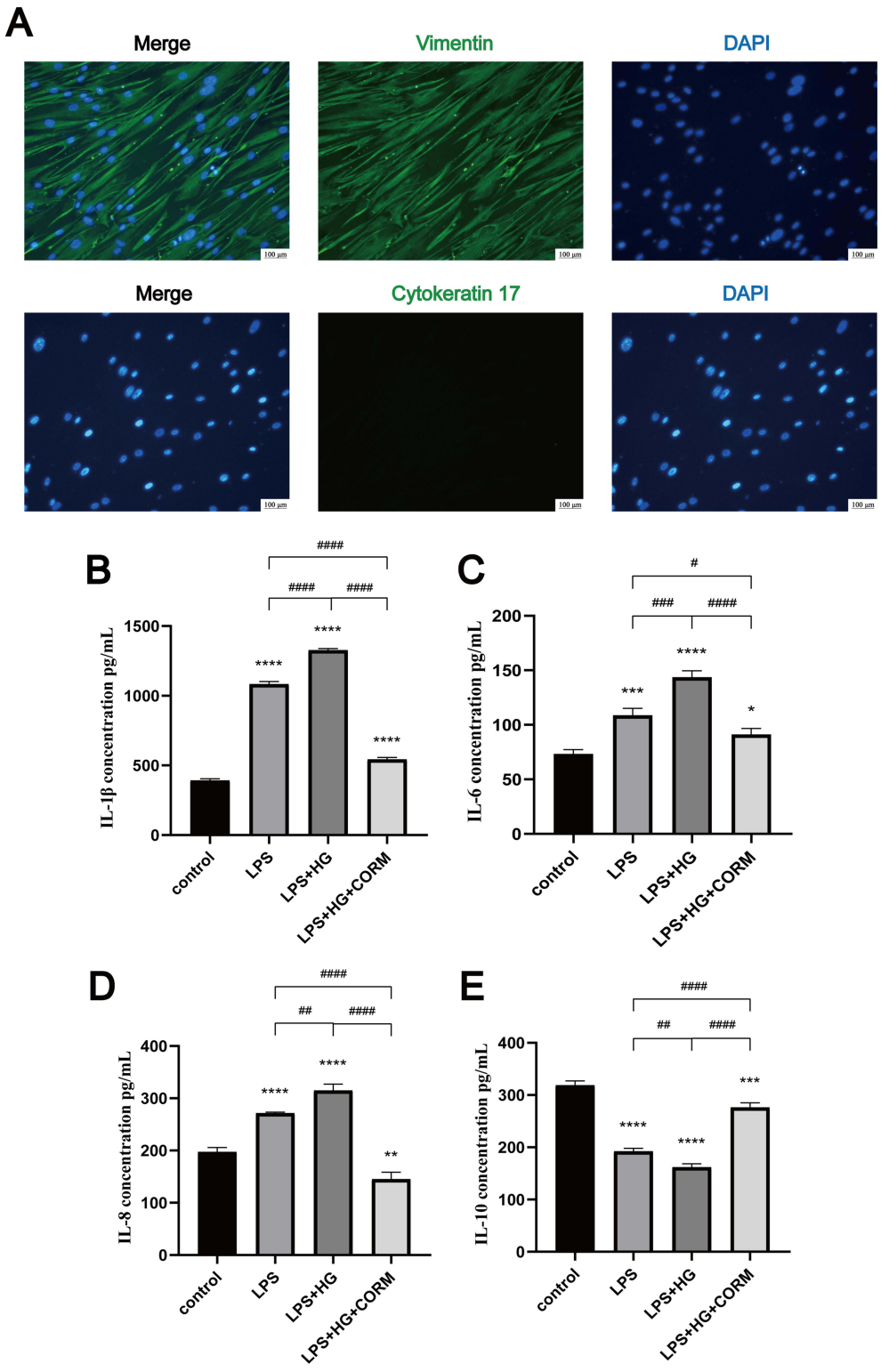

Figure 1 CORM-3 reduces LPS-induced release of inflammatory cytokines from hPDLCs in the presence of high glucose.

Notes: (**A**) hPDLCs were fixed with 4% Paraformaldehyde and incubated with vimentin and keratin antibody. Goat anti-rabbit IgG (Alexa Fluor® 488) was used as the secondary antibody. Nuclei were stained blue with DAPI. Images were taken with a Zeiss LSM 880 laser-scanning microscope (Carl Zeiss, Oberkochen, Germany). (**B**–**E**) hPDLCs were divided into 4 groups as follows: Control group, in which the cells were cultured in control medium (cell growing medium containing 5.6 mM D-glucose); LPS treatment group, in which the cells were incubated in control medium containing 10 μg/mL LPS; LPS + high glucose co-treatment group, in which the cells were cotreated with high glucose medium (45 mM D-glucose) containing 10 μg/mL LPS; LPS + high glucose + CORM-3 group, in which the cells were pretreated with CORM-3 (400 μM) for 24 h prior to incubation in high glucose medium (45 mM D-glucose) containing 10 μg/mL LPS. IL-1β, IL-6, IL-8 and IL-10 concentrations were determined by ELISA kit among 4 groups. Data were presented as mean ± SD. $^{\#}p<0.05$, $^{\#\#}p<0.01$, $^{\#\#\#}p<0.001$, $^{\#\#\#\#}p<0.0001$ vs experimental groups; $^{*}p<0.05$, $^{**}p<0.01$, $^{***}p<0.001$, $^{****}p<0.0001$ vs control group.

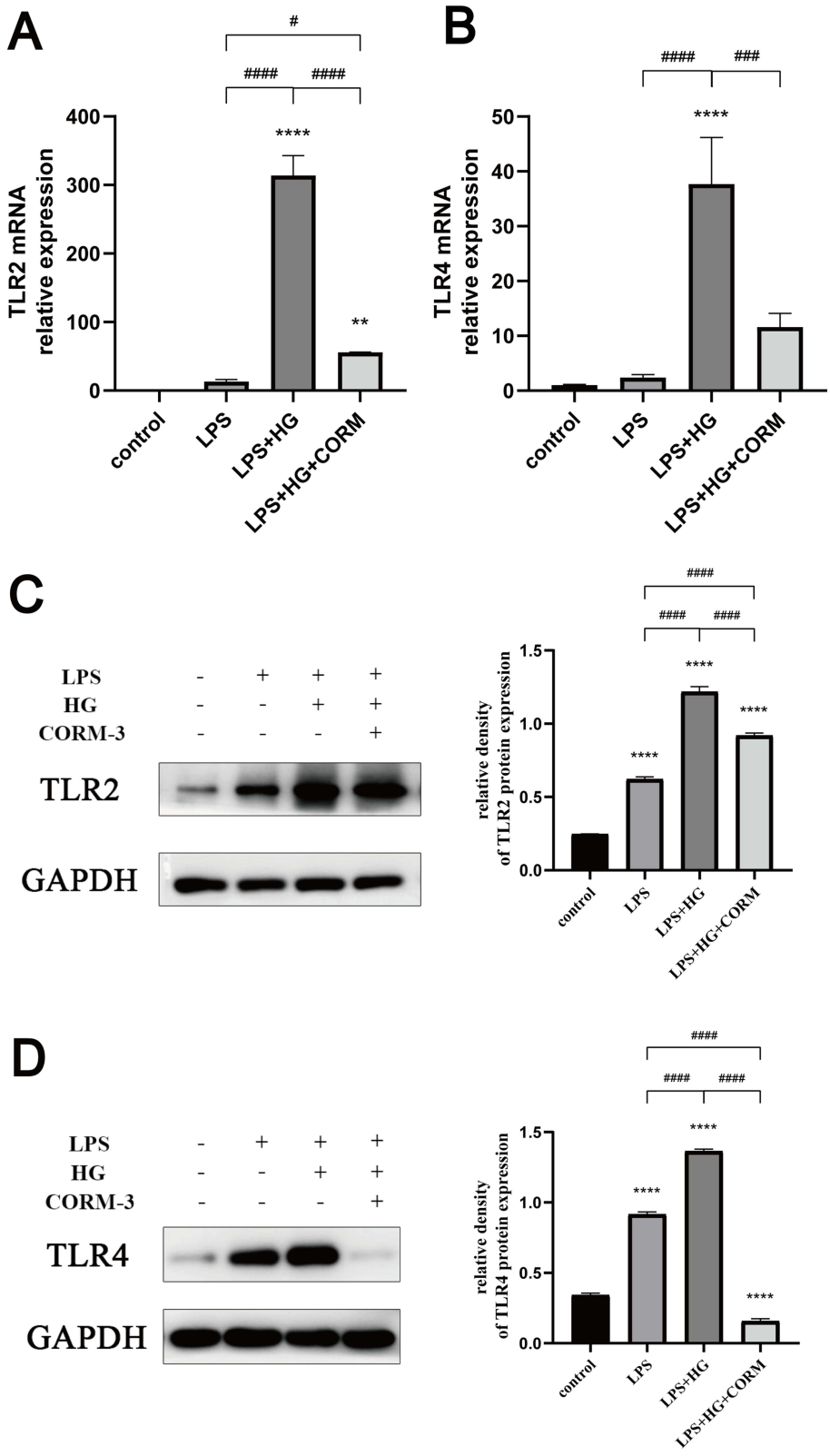

Figure 2 CORM-3 reduces LPS-induced TLR-2 and TLR-4 expression in hPDLCs in the presence of high-glucose.

Notes: hPDLCs were divided into 4 groups as follows: Control group, in which the cells were cultured in control medium (cell growing medium containing 5.6 mM D-glucose); LPS treatment group, in which the cells were incubated in control medium containing 10 μg/mL LPS; LPS + high glucose co-treatment group, in which the cells were cotreated with high glucose medium (45 mM D-glucose) containing 10 μg/mL LPS; LPS + high glucose + CORM-3 group, in which the cells were pretreated with CORM-3 (400 μM) for 24 h prior to incubation in high glucose medium (45 mM D-glucose) containing 10 μg/mL LPS. mRNA expressions of TLR2 (**A**) and TLR4 (**B**) were detected by RT-qPCR among 4 groups above. Protein expressions of TLR2 (**C**) and TLR4 (**D**) were measured by Western Blot among 4 groups above. Data were presented as mean ± SD. $^{\#}p<0.05$, $^{\#\#\#\#}p<0.001$, $^{\#\#\#\#\#}p<0.0001$ vs experimental groups; $^{**}p<0.01$, $^{****}p<0.0001$ vs control group.

CORM-3 Reduces LPS-Induced RAGE Expression and NF-κB Pathway Activation in the Presence of High Glucose

RT-qPCR and Western blot analysis showed that both the mRNA and protein expression of the surface receptor RAGE stimulated with LPS were significantly increased compared with that in control group (Figure 3A and D). The mRNA expression of its downstream molecule MyD88 was also significantly increased with LPS stimulation (Figure 3B). With the co-stimulation of LPS and high glucose, the expression of RAGE mRNA and protein was significantly higher than that of LPS group. The mRNA expression of its downstream molecule MyD88 was also significantly increased. These results indicated that the high glucose environment significantly increased the expression of RAGE. However, after CORM-3 pretreatment, both the mRNA and protein expression of RAGE stimulated with LPS and high glucose decreased significantly. Meanwhile, we confirm that CORM-3 per se has no effect on the expression of RAGE (Figure S5). The mRNA expression of its downstream molecule MyD88 was also significantly reduced by CORM-3. As for NF-κB pathway, the mRNA and protein expression of the molecule IκBα, p65 and p50 increased significantly in the presence of LPS and high glucose, and the expression of their phosphorylated proteins P-IκBα, P-p65 and P-p50 also increased significantly (Figure 3C and E), indicating the activation of NF-κB pathway. After pretreatment with CORM-3, the expression of these NF-κB pathway-related factors induced with LPS and high glucose was significantly inhibited. The same trend was also demonstrated in the expression of phosphorylated proteins P-IκBα, P-p65 and P-p50.

The Modulatory Effect of CORM-3 on the Expression of TLR2 and TLR4 and NF-κB Pathway-Related Factors After RAGE Silencing or Overexpression

RT-qPCR and Western blot were used to detect the transfection efficiency by examining the mRNA and protein expression of RAGE after transfection. The mRNA and protein expression of RAGE decreased significantly in RAGE siRNA transfected cells, and increased significantly in RAGE overexpression plasmid transfected cells. No significant difference between the transfected NC group and the blank control group was found, indicating that the transfection experiment per se had no effect on the expression of each factor, as shown in Figures 4A and 5A.

RAGE siRNA transfection significantly decreased the mRNA and protein expression of TLR2, TLR4, MyD88, IκBα, p65 and p50. The expression of the factors described above in the silent+CORM group also decreased, showing the important role of RAGE in LPS- and high glucose-induced response. Nevertheless, there was no statistical difference in the expression of the factors in the transfected cells in the presence or absence of CORM-3, suggesting that the effect of CORM-3 was abrogated in the absence of RAGE. The expression of phosphorylated protein P-IκBα, P-p65 and P-p50 decreased significantly in cells transfected with RAGE siRNA, indicating that RAGE silencing significantly inhibited the activation of NF-κB pathway (Figure 4B and C).

RAGE overexpression vector plasmid transfection significantly enhanced the mRNA and protein expression of TLR2, TLR4, MyD88, IκBα, p65 and p50. CORM-3 significantly reduced the expression of RAGE and the expression level of above factors in RAGE overexpressed cells (Figure 5B and C). Immunohistochemical staining showed the translocation of NFκB-p65 into the nucleus in cells of the control group and NC group, but no nuclear translocation of p65 was found in NC+CORM group, silent group, and silent+CORM group (Figure 4D). CORM-3 significantly inhibited RAGE-induced NFκB-p65 nuclear transport (Figure 5D).

CORM-3 Suppresses the Inflammatory Response of Periodontal Tissues in Experimental Periodontitis of Diabetic Rats

The blood glucose index of every group were detected after completing STZ injection cycle (Figure S6). In the healthy group, the gingival sulcus floor was located at the neck of the tooth, and the gingival epithelium, the epithelium in the sulcus, and the junctional epithelium were intact, the epithelial nail processes were short and neat, and the alveolar bone below was not obviously absorbed. In CP group and DM+CP group, attachment loss occurred. The bottom of the periodontal pocket was located in the middle 1/3 of the root. Gingival hyperplasia was soft. The gingival epithelium and the inner wall epithelium of the periodontal pocket were damaged discontinuously. The epithelial nail process was elongated and irregular after inflammatory stimulation. Alveolar bone resorption occurred. There were inflammatory cells

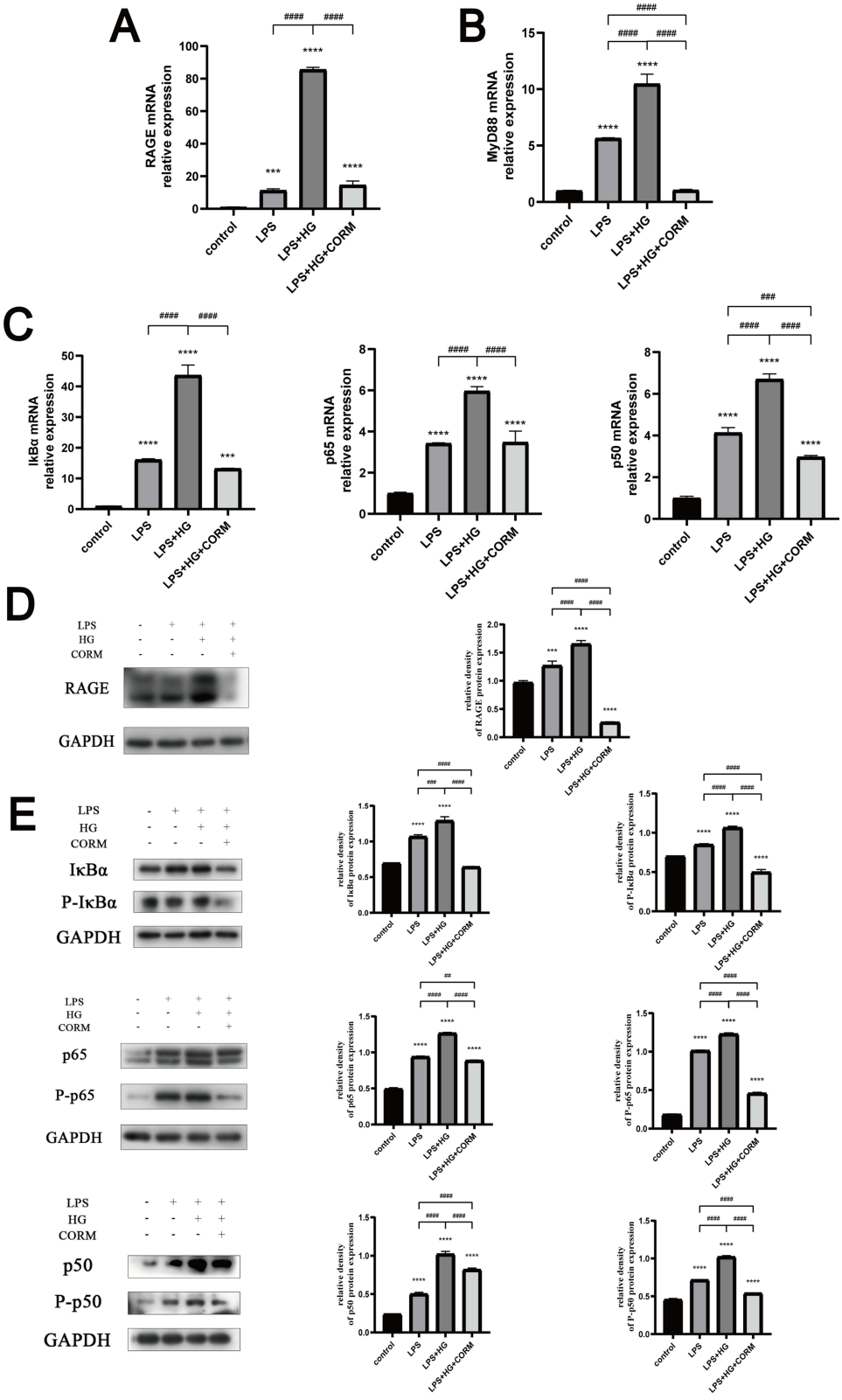

Figure 3 CORM-3 reduces high-glucose-promoted RAGE expression and NF-κB pathway activation in LPS-induced hPDLCs.

Notes: hPDLCs were divided into 4 groups as follows: Control group, in which the cells were cultured in control medium (cell growing medium containing 5.6 mM D-glucose); LPS treatment group, in which the cells were incubated in control medium containing 10 μg/mL LPS; LPS + high glucose co-treatment group, in which the cells were cotreated with high glucose medium (45 mM D-glucose) containing 10 μg/mL LPS; LPS + high glucose + CORM-3 group, in which the cells were pretreated with CORM-3 (400 μM) for 24 h prior to incubation in high glucose medium (45 mM D-glucose) containing 10 μg/mL LPS. mRNA expressions of RAGE (**A**), MyD88 (**B**) and NF-κB pathway molecules (**C**) were detected by qRT-qPCR among 4 groups above. Protein expressions of RAGE (**D**) and NF-κB pathway molecules (**E**) were measured by Western Blot among 4 groups above. Data were presented as mean ± SD. $^{\#\#}p<0.01$, $^{\#\#\#\#}p<0.001$, $^{\#\#\#\#\#}p<0.0001$ vs experimental groups; $^{***}p<0.001$, $^{****}p<0.0001$ vs control group.

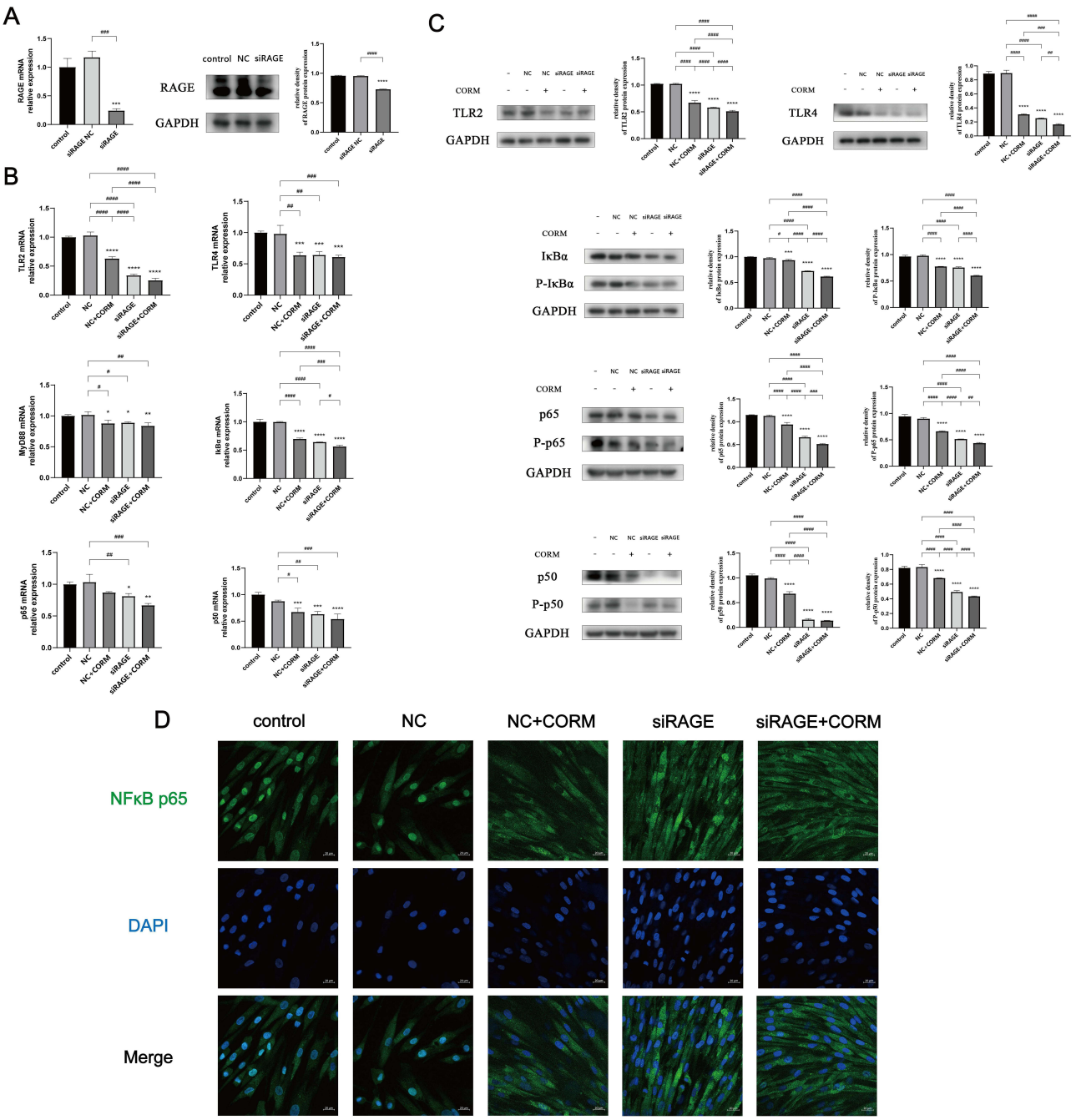

Figure 4 The modulatory effect of CORM-3 on the expression of TLR2 and TLR4 and NF-κB pathway-related factors after RAGE silencing.

Notes: hPDLCs were divided into 5 groups: Control group, in which the cells were incubated with medium containing 10 μg/mL LPS and 45 mM D-glucose; siRNA NC, in which the cells were transfected with siRNA NC and incubated with LPS and high glucose; siRNA NC + CORM group, in which the cells were transfected with siRNA NC and incubated with LPS, high glucose and 400 μM CORM-3; RAGE siRNA group, in which the RAGE siRNA transfected cells were incubated with LPS and high glucose; RAGE siRNA + CORM group, in which RAGE siRNA transfected cells were incubated with LPS, high glucose and CORM-3. (**A**) RAGE specific siRNA constructed in vitro was successfully transfected into hPDLCs. (**B**) mRNA expressions of TLR-2, TLR-4, MyD88 and NF-κB pathway molecules after RAGE silencing were detected by RT-qPCR. (**C**) Protein expressions of TLR-2, TLR-4, MyD88 and NF-κB pathway molecules after RAGE silencing were measured by Western Blot. (**D**) Immunofluorescence showed the nuclear penetration of NFκB-p65. Data were presented as mean ± SD. $^{\#}p<0.05$, $^{\#\#}p<0.01$, $^{\#\#\#}p<0.001$, $^{\#\#\#\#}p<0.0001$ vs experimental groups; $^{*}p<0.05$, $^{**}p<0.01$, $^{***}p<0.001$, $^{****}p<0.0001$ vs control group.

in the lamina propria but not obvious. In CORM+DM+CP group, attachment loss and alveolar bone resorption also existed, the epithelium was complete and continuous, the epithelial nail process was thickened and orderly, and no obvious inflammatory cells were found in the lamina propria (Figure 6A). We measured attachment loss based on HE staining slices (Figure S7). Collagen fibers proliferated in the lamina propria of CP group compared with that in the

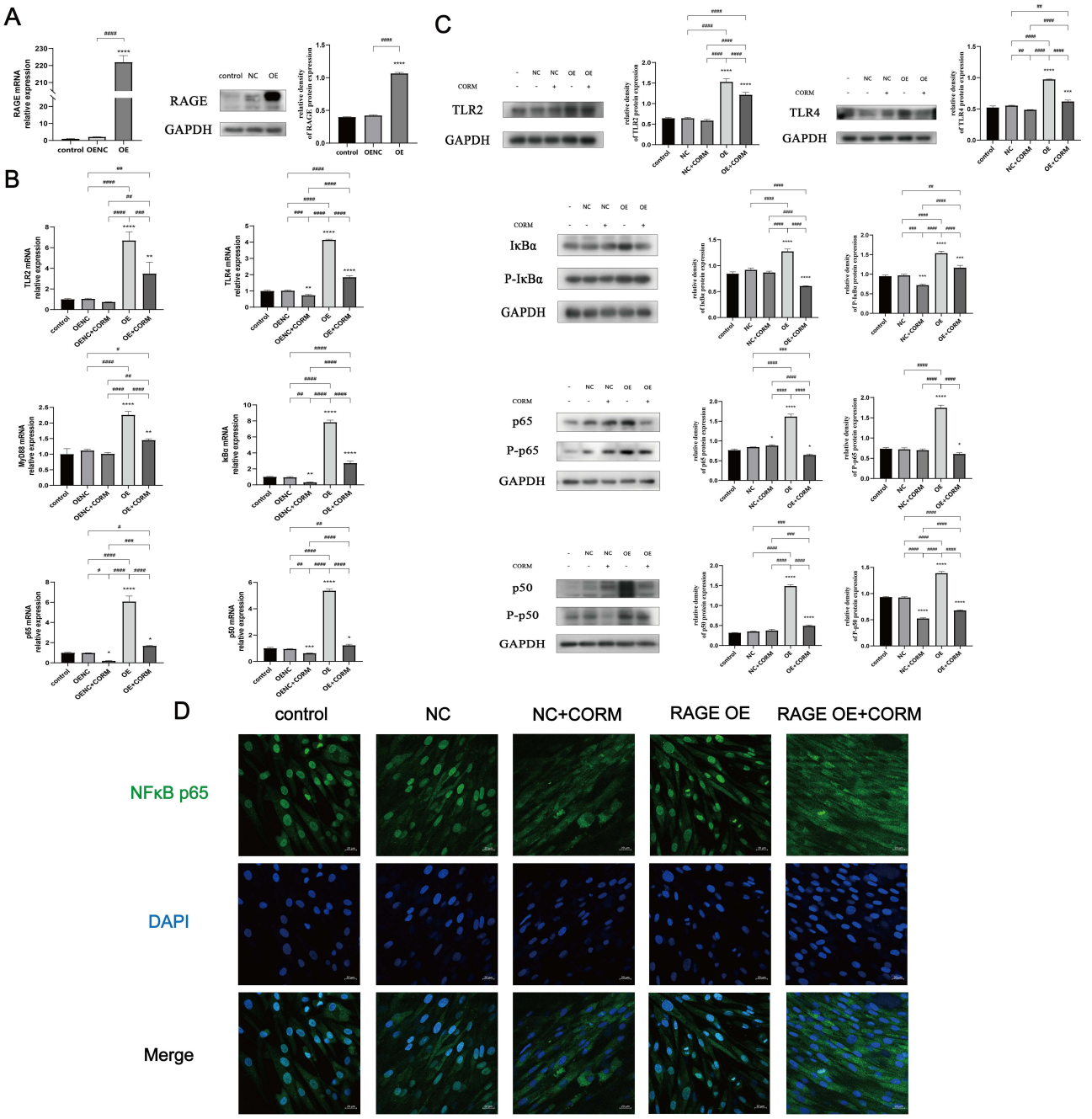

Figure 5 CORM-3 reduces the expression of receptors and pathway-related molecules after RAGE overexpression.

Notes: hPDLCs were divided into 5 groups: Control group, in which the cells were incubated with medium containing 10 μg/mL LPS and 45 mM D-glucose; empty vector group, in which the cells were transfected with empty vector and incubated with LPS and high glucose; empty vector + CORM group, in which the cells were transfected with empty vector and incubated with LPS, high glucose and 400 μM CORM-3; RAGE overexpression group, in which the RAGE overexpression vector transfected cells were incubated with LPS and high glucose; RAGE overexpression + CORM group, in which RAGE overexpression vector transfected cells were incubated with LPS, high glucose and CORM-3. (**A**) RAGE specific overexpression vector constructed in vitro was successfully transfected into hPDLCs. (**B**) mRNA expressions of TLR-2, TLR-4, MyD88 and NF-κB pathway molecules after RAGE overexpression were detected by RT-qPCR. (**C**) Protein expressions of TLR-2, TLR-4, MyD88 and NF-κB pathway molecules after RAGE overexpression were measured by Western Blot. (**D**) Immunofluorescence showed the nuclear penetration of NFκB-p65. Data were presented as mean ± SD. $^{\#}p<0.05$, $^{\#\#}p<0.01$, $^{\#\#\#}p<0.001$, $^{\#\#\#\#}p<0.0001$ vs experimental groups; $^{*}p<0.05$, $^{**}p<0.01$, $^{***}p<0.001$, $^{****}p<0.0001$ vs control group.

healthy group. Collagen fibers proliferated more significantly in DM+CP group than in CP group. The degree of blue staining in the lamina propria of CORM+DM+CP group was similar to that of the healthy group, and there was no obvious collagen fiber proliferation (Figure 6B).

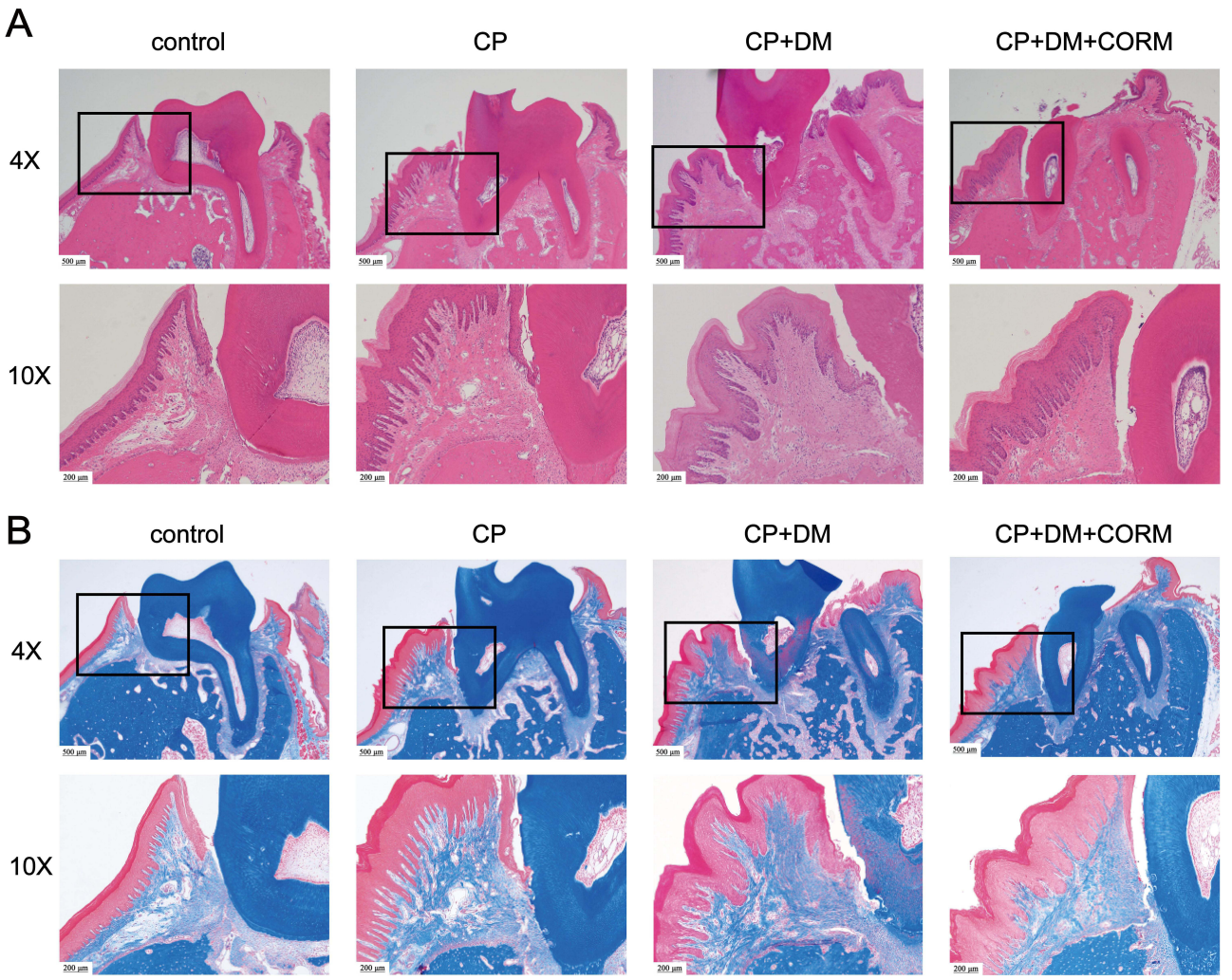

Figure 6 CORM-3 suppresses the inflammatory response in experimental periodontitis of diabetic rats.
Notes: The rats were divided into 4 groups as follows: Control group, healthy rats without any treatment; Chronic periodontitis (CP) group, experimental periodontitis rat model; Diabetes mellitus (DM) + CP group, experimental periodontitis model in diabetes rats; CORM + DM + CP group, experimental periodontitis model in diabetes rats, CORM-3 solution (10 mg/kg) was injected intraperitoneally every other day. Two weeks after the establishment of periodontitis, the maxillary tissues were isolated. HE and Masson staining was applied to examine the inflammatory response of periodontal tissues of the rats. (**A**) HE staining showed the inflammation of periodontal tissue. (**B**) Masson staining showed fibroproliferation.

Immunohistochemistry showed that RAGE was expressed in the upper cortex of healthy rats to a certain extent. RAGE expression was found in the entire epithelial layer of CP group rats, and there was no significant difference compared with the healthy group. RAGE expression in DM+CP group was significantly increased compared with that in CP group and healthy group. CORM-3 treatment significantly suppressed the RAGE expression in periodontal tissues in diabetes rats with experimental periodontitis. RAGE expression was concentrated on the surface of granular layer and acanthous layer, while RAGE expression in basal layer was weak (Figure 7A).

Immunofluorescence showed that NF-κB p65 was much expressed in periodontal tissue in CP group and DM+CP group than in control group, but decreased in CORM+DM+CP group (Figure 7B).

Discussion and Conclusion

Hyperglycemia is associated with increased severity of periodontitis and poor periodontal outcomes even after periodontal therapy. In the present study, we demonstrated that high-glucose concentrations aggravated LPS-induced cell viability decrease and upregulated LPS-induced inflammatory response in hPDLCs, while CORM-3 effectively reversed the adverse impacts on hPDLCs imposed by LPS and high glucose. Our results showed that in addition to the positive

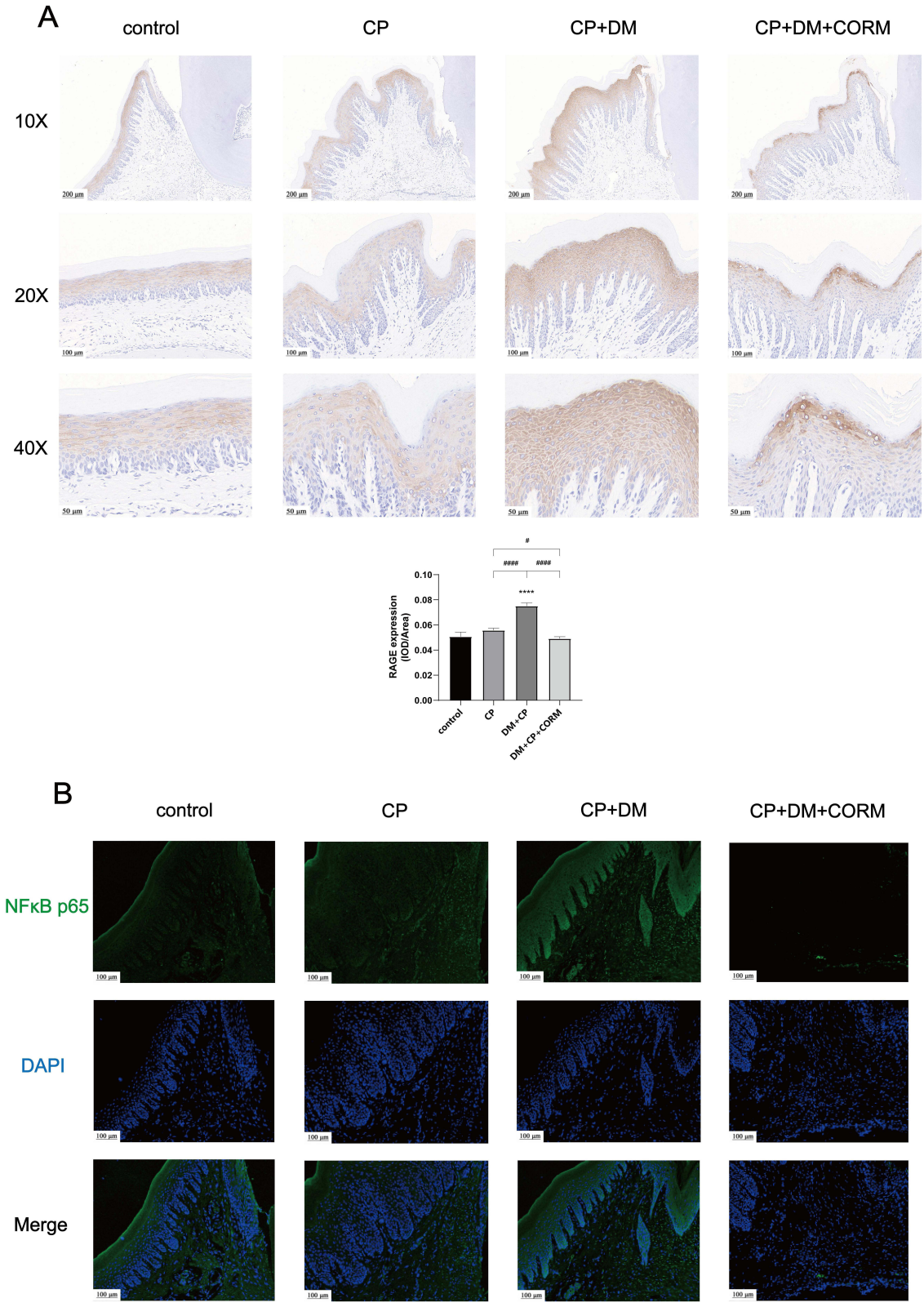

Figure 7 CORM-3 reduced the expression of RAGE and NFκB-p65 in experimental periodontitis of diabetic rats.

Notes: The rats were divided into 4 groups as follows: Control group, healthy rats without any treatment; Chronic periodontitis (CP) group, experimental periodontitis rat model; Diabetes mellitus (DM) + CP group, experimental periodontitis model in diabetes rats; CORM + DM + CP group, experimental periodontitis model in diabetes rats, CORM-3 solution (10 mg/kg) was injected intraperitoneally every other day. Two weeks after the establishment of periodontitis, Immunohistochemical staining was used to detect the expression of RAGE and NF-κB p65. (**A**) Immunohistochemical staining of RAGE showed the expression of RAGE in periodontal tissue. (**B**) Immunofluorescence showed the expression of p65 in periodontal tissue. Data were presented as mean ± SD. $^{\#}p<0.05$, $^{\#\#\#\#}p<0.0001$ vs experimental groups; $^{****}p<0.0001$ vs control group.

effects exerted by CORM-3 against inflammatory response in LPS-treated hPDLCs, this compound also plays an anti-inflammation role in hPDLCs under hyperglycemic conditions.

A blood glucose concentration beyond 5.6 mM is regard as diabetes according to the criteria from American Diabetes Association.[38] Clinical studies showed that blood glucose levels among diabetes patients have a wide distribution, ranging from 5.6 mM to even 60 mM.[39] It has been reported that 25 mM glucose treatment significantly impaired the cell viability of hPDLCs.[40] Therefore, in the present study, a concentration of 45 mM was considered as high-glucose and 5.6 mM was used as control.

High levels of glucose have been reported to suppress viability of periodontal ligament fibroblasts and increase apoptosis of these cells,[41,42] which is reconfirmed by our results that the proliferation of hPDLCs in LPS+HG group was further inhibited compared with in LPS group. More importantly, as one of the primary effects of diabetes on periodontal tissue, highly upregulated inflammation directly contributes to periodontal ligament destruction and alveolar bone resorption. In the present study, high glucose significantly increased inflammation, as evidenced by enhanced levels of pro-inflammation cytokines including IL-1β, IL-6 and IL-8. In periodontitis patients with poorly controlled diabetes, the level of pro-inflammatory factors such as IL-1β, IL-6 and IL-8 in gingiva is significantly increased, and the level of anti-inflammatory factors such as IL-10 in gingiva is significantly decreased, which may be one of the ways that diabetes aggravates periodontitis.[43] Mechanistic links between periodontitis and diabetes involve elevations in IL-1β, tumour necrosis factor-α, IL-6, receptor activator of NFκB ligand/osteoprotegerin ratio, oxidative stress and TLR2/4 expression.[44]

Exogenous CO has been reported to protect many tissues, including cardiovascular, respiratory and digestive systems, against ischemia/reperfusion injury by its anti-ischemic and anti-inflammatory activities.[45–47] Our previous study indicated that CORM-2, another member of CORMs, reduced periodontal inflammation and alveolar bone loss in rat model of experimental periodontitis.[48] As a consequence, CORM-3 might be of therapeutic interest by delivering CO in precise amounts to periodontal tissue in a controllable manner. In the absence of extensive experimental evidence, the potential toxic effect of CORM-3 on hPDLCs remains unclear. Based on the results of our previous studies, a concentration of CORM-3 at 800 μM significantly inhibited cell viability, and 400 μM CORM-3 inhibited the expression of LPS-induced inflammatory cytokines without cytotoxicity to cells. A 400 μM was therefore selected as an appropriate concentration for CORM-3 in this study.

TLR2 and TLR4 are important immune-related transmembrane proteins expressed by various cell types including hPDLCs.[49] They recognize pathogen-associated molecular patterns (PAMPs) including LPS and induce the production of proinflammatory cytokines via several signaling pathways, which activates hosts' immune response to periodontal pathogenic agents.[50,51] Here, we show that high glucose increased LPS-induced TLR2 and TLR4 expression, while CORM-3 pretreatment significantly prohibits the increase of TLR2/4 on hPDLCs in LPS+HG group. Considering the facts that TLRs function upstream of inflammatory cytokines, and the suppression of TLR2/4 expression by CORM-3, it is supposed that CORM-3 inhibits inflammation by decreasing the expression of TLR-2 and TLR-4 on hPDLCs.

A number of researches show that RAGE plays an important role in LPS-induced NFκB activation and endothelial barrier dysfunction.[52] Further studies showed that overexpression of NAG-1/GDF15 could suppress renal and systemic inflammation in mice, decreased AGE/RAGE axis related downstream inflammatory molecules and adhesion molecules, and inhibited the activation of TLR4/MyD88/NFκB signal pathway.[53] In addition, there is accumulated evidence showing a synergistic interaction between RAGE and TLR family in host immune response. RAGE and TLR share three ligands, HMGB, S100 and LPS. Though the mechanism or physicochemical conditions for selecting ligands to preferentially bind RAGE or TLR are not clear, more and more evidences support their potential synergistic effects on downstream signaling pathways and the results of these interactions on inflammatory response.[54] High concentrations of AGEs are considered as endogenous "danger signals", which lead to the activation of TLR/MyD88/NFκB pathway and further aggravates the inflammatory response combined with the receptor RAGE. The expression of TLR-2 and TLR-4 was up-regulated by AGE-RAGE axis, and MyD88 signal pathway was induced. This further activates the inflammatory mediator NFκB pathway, which mediates the secretion of pro-inflammatory cytokines.[55]

In order to explore the possible mechanism, we investigated TLR2/TLR4/NF-κB pathway and AGE/RAGE/NF-κB pathway in consideration of the related signal pathways stimulated by LPS and high glucose. Our data showed that CORM-3 had a significant inhibitory effect on the inflammatory pathway after RAGE silencing. In the RAGE overexpression

transfection experiment, CORM-3 significantly inhibited the activation of NF-κB pathway enhanced by RAGE overexpression. At the same time, overexpression of RAGE induced the increase of the expression of TLR2 and TLR4. Based on the data that overexpression of RAGE promoted the expression of TLR2 and TLR4, it can be speculated that high glucose may work with LPS, resulting in a synergistic effect on the expression of TLR2 and TLR4, and RAGE. Two pathways jointly promote LPS and high glucose-induced hPDLCs inflammatory response. CORM-3 reduces the activation of NF-κB pathway by downregulating the expression of TLR2, TLR4, and RAGE, which can inhibit inflammation. It cannot be ruled out that NF-κB pathway is enhanced by high expression of RAGE and there is feedback regulation on the expression of TLR2 and TLR4, so it is worth further discussing the crosstalk between TLR2/TLR4/NF-κB pathway and AGE/RAGE/NF-κB pathway. It is worth further exploring whether the reduction of TLRs expression after RAGE knockdown is a direct or indirect effect, and whether the silence of TLRs affects RAGE expression. CORM-3 has a significant inhibitory effect on this crosstalk, but the specific action site and the upstream–downstream relationship are still unclear. The exact mechanism by which CORM-3 functions within cells and affects TLRs, RAGE, and NF-κB pathway remains unclear.

The inhibitory effect of CORM-3 on inflammation was demonstrated to be mediated by release of CO, which has been shown in a variety of cell types.[56] Our unpublished data also revealed that deactivated CORM-3, which is prepared by dissolving CORM-3 in water for more than 24 h, did not suppress inflammatory response of hPDLCs induced by LPS and high glucose. Moreover, another study of our research team showed that heme oxygenase-1 (HO-1) pathway was tightly involved in CORM-3 mediated anti-inflammation effect in hPDLCs. Mitogen-activated protein kinase (MAPK) and glutathione signaling pathways have also been pointed to participate in physiological roles of CO.[57]

In conclusion, our data show that LPS-induced decline in cell proliferation and increase in inflammatory response in hPDLCs are further aggravated by high glucose treatment. The pretreatment of CORM-3 significantly inhibited the enhanced inflammatory response of hPDLCs induced by LPS and high glucose. These results suggest CORM-3 as a new therapeutic strategy for the treatment of inflammatory periodontal diseases.

Ethics Approval and Informed Consent

According to the Helsinki Declaration, all participants provided written informed consent, and patients under the age of 18 received written informed consent from their parents. The study has been approved by the Ethics Committee of Shandong University Stomatological Hospital.

Ethics Approval and Consent to Participate

All guidelines on animal care and use applicable to international, national and/or institutions have been complied with.

Acknowledgments

The present study was supported by Shandong Provincial Natural Science Foundation (ZR2020MH186), Shandong Provincial Science and Technology Development Plan (2010GSF10270).

Disclosure

The authors declare no conflicts of interest in this work.

References

1. Kinane DF, Stathopoulou PG, Papapanou PN. Periodontal diseases. *Nat Rev Dis Primers*. 2017;3(1):17038. doi:10.1038/nrdp.2017.38
2. Pihlstrom BL, Michalowicz BS, Johnson NW. Periodontal diseases. *Lancet*. 2005;366(9499):1809–1820. doi:10.1016/S0140-6736(05)67728-8
3. Wu CZ, Yuan YH, Liu HH, et al. Epidemiologic relationship between periodontitis and type 2 diabetes mellitus. *BMC Oral Health*. 2020;20(1):204. doi:10.1186/s12903-020-01180-w
4. Romano F, Perotto S, Mohamed SEO, et al. Bidirectional association between metabolic control in type-2 diabetes mellitus and periodontitis inflammatory burden: a cross-sectional study in an Italian Population. *J Clin Med*. 2021;10(8):1787. doi:10.3390/jcm10081787
5. Li Y, Du Z, Xie X, et al. Epigenetic changes caused by diabetes and their potential role in the development of periodontitis. *J Diabetes Investig*. 2021;12(8):1326–1335. doi:10.1111/jdi.13477
6. Joseph R, Sasikumar M, Mammen J, Joseraj MG, Radhakrishnan C. Nonsurgical periodontal-therapy improves glycosylated hemoglobin levels in pre-diabetic patients with chronic periodontitis. *World J Diabetes*. 2017;8(5):213–221. doi:10.4239/wjd.v8.i5.213

7. Teshome A, Yitayeh A. The effect of periodontal therapy on glycemic control and fasting plasma glucose level in type 2 diabetic patients: systematic review and meta-analysis. *BMC Oral Health*. 2016;17(1):31. doi:10.1186/s12903-016-0249-1
8. Cao R, Li Q, Wu Q, Yao M, Chen Y, Zhou H. Effect of non-surgical periodontal therapy on glycemic control of type 2 diabetes mellitus: a systematic review and Bayesian network meta-analysis. *BMC Oral Health*. 2019;19(1):176. doi:10.1186/s12903-019-0829-y
9. Graves DT, Ding Z, Yang Y. The impact of diabetes on periodontal diseases. *Periodontol*. 2000;82(1):214–224. doi:10.1111/prd.12318
10. Nibali L, Gkranias N, Mainas G, Di Pino A. Periodontitis and implant complications in diabetes. *Periodontol*. 2022;90(1):88–105. PMID: 35913467; PMCID: PMC9805043. doi:10.1111/prd.12451
11. Reichert S, Hofmann B, Kohnert M, et al. Advanced Glycation End Product (AGE) and Soluble Receptor of AGE (sRAGE) Levels in Relation to Periodontitis Severity and as Putative 3-Year Outcome Predictors in Patients Undergoing Coronary Artery Bypass Grafting (CABG). *J Clin Med*. 2022;11(14):4105. PMID: 35887868; PMCID: PMC9317367. doi:10.3390/jcm11144105
12. Teissier T, Boulanger É. The receptor for advanced glycation end-products (RAGE) is an important pattern recognition receptor (PRR) for inflammaging. *Biogerontology*. 2019;20(3):279–301. doi:10.1007/s10522-019-09808-3
13. Kim HJ, Jeong MS, Jang SB. Molecular characteristics of RAGE and advances in small-molecule inhibitors. *Int J Mol Sci*. 2021;22(13):6904. PMID: 34199060; PMCID: PMC8268101. doi:10.3390/ijms22136904
14. Watanabe H, Son M. The immune tolerance role of the HMGB1-RAGE axis. *Cells*. 2021;10(3):564. PMID: 33807604; PMCID: PMC8001022. doi:10.3390/cells10030564
15. Du C, Whiddett RO, Buckle I, Chen C, Forbes JM, Fotheringham AK. Advanced glycation end products and inflammation in type 1 diabetes development. *Cells*. 2022;11(21):3503. PMID: 36359899; PMCID: PMC9657002. doi:10.3390/cells11213503
16. Khalid M, Petroianu G, Adem A. Advanced glycation end products and diabetes mellitus: mechanisms and perspectives. *Biomolecules*. 2022;12(4):542. PMID: 35454131; PMCID: PMC9030615. doi:10.3390/biom12040542
17. Twarda-Clapa A, Olczak A, Białkowska AM, Koziołkiewicz M. Advanced Glycation End-Products (AGEs): formation, chemistry, classification, receptors, and diseases related to AGEs. *Cells*. 2022;11(8):1312. PMID: 35455991; PMCID: PMC9029922. doi:10.3390/cells11081312
18. Amin R, Indiarsih TB, Sari PM, Purwanita P. Anti-RAGE (Receptor Advanced Glycation End products) antibody improves diabetic retinopathy in rats via hypoglycemic and anti-inflammatory mechanism. *Rep Biochem Mol Biol*. 2022;11(3):394–399. PMID: 36718309; PMCID: PMC9883039. doi:10.52547/rbmb.11.3.394
19. Weider M, Schröder A, Docheva D, et al. A human periodontal ligament fibroblast cell line as a new model to study periodontal stress. *Int J Mol Sci*. 2020;21(21):7961. doi:10.3390/ijms21217961
20. Kato H, Taguchi Y, Tominaga K, et al. High glucose concentrations suppress the proliferation of human periodontal ligament stem cells and their differentiation into osteoblasts. *J Periodontol*. 2016;87(4):e44–e51. doi:10.1902/jop.2015.150474
21. Zhu W, Qiu Q, Luo H, et al. High glucose exacerbates TNF-α-induced proliferative inhibition in human periodontal ligament stem cells through upregulation and activation of TNF receptor 1. *Stem Cells Int*. 2020;2020:4910767. doi:10.1155/2020/4910767
22. Ismailova A, Kuter D, Bohle DS, Butler IS. An overview of the potential therapeutic applications of CO-releasing molecules. *Bioinorg Chem Appl*. 2018;2018:8547364. doi:10.1155/2018/8547364
23. Queiroga CS, Vercelli A, Vieira HL. Carbon monoxide and the CNS: challenges and achievements. *Br J Pharmacol*. 2015;172(6):1533–1545. doi:10.1111/bph.12729
24. Ryter SW, Choi AM. Targeting heme oxygenase-1 and carbon monoxide for therapeutic modulation of inflammation. *Transl Res*. 2016;167(1):7–34. doi:10.1016/j.trsl.2015.06.011
25. McRae KE, Pudwell J, Peterson N, Smith GN. Inhaled carbon monoxide increases vasodilation in the microvascular circulation. *Microvasc Res*. 2019;123:92–98. doi:10.1016/j.mvr.2019.01.004
26. Segersvärd H, Lakkisto P, Hänninen M, et al. Carbon monoxide releasing molecule improves structural and functional cardiac recovery after myocardial injury. *Eur J Pharmacol*. 2018;818:57–66. doi:10.1016/j.ejphar.2017.10.031
27. Ryter SW. Therapeutic potential of heme oxygenase-1 and carbon monoxide in acute organ injury, critical illness, and inflammatory disorders. *Antioxidants*. 2020;9(11):1153. doi:10.3390/antiox9111153
28. Southam HM, Smith TW, Lyon RL, et al. A thiol-reactive Ru(II) ion, not CO release, underlies the potent antimicrobial and cytotoxic properties of CO-releasing molecule-3. *Redox Biol*. 2018;18:114–123. doi:10.1016/j.redox.2018.06.008
29. Wilson JL, Jesse HE, Hughes B, et al. Ru(CO)3Cl(Glycinate) (CORM-3): a carbon monoxide-releasing molecule with broad-spectrum antimicrobial and photosensitive activities against respiration and cation transport in Escherichia coli. *Antioxid Redox Signal*. 2013;19(5):497–509. doi:10.1089/ars.2012.4784
30. Riquelme SA, Bueno SM, Kalergis AM. Carbon monoxide down-modulates Toll-like receptor 4/MD2 expression on innate immune cells and reduces endotoxic shock susceptibility. *Immunology*. 2015;144(2):321–332. doi:10.1111/imm.12375
31. Schatzschneider U. Novel lead structures and activation mechanisms for CO-releasing molecules (CORMs). *Br J Pharmacol*. 2015;172(6):1638–1650. doi:10.1111/bph.12688
32. Guo Y, Stein AB, Wu W-J, et al. Administration of a CO-releasing molecule at the time of reperfusion reduces infarct size in vivo. *Am J Physiol Heart Circ Physiol*. 2004;286(5):H1649–H1653. doi:10.1152/ajpheart.00971.2003
33. Masini E, Vannacci A, Failli P, et al. A carbon monoxide-releasing molecule (CORM-3) abrogates polymorphonuclear granulocyte-induced activation of endothelial cells and mast cells. *FASEB J*. 2008;22(9):3380–3388. doi:10.1096/fj.08-107110
34. Jiang L, Fei D, Gong R, et al. CORM-2 inhibits TXNIP/NLRP3 inflammasome pathway in LPS-induced acute lung injury. *Inflamm Res*. 2016;65(11):905–915. PMID: 27412237. doi:10.1007/s00011-016-0973-7
35. Song L, Li J, Yuan X, et al. Carbon monoxide-releasing molecule suppresses inflammatory and osteoclastogenic cytokines in nicotine- and lipopolysaccharide-stimulated human periodontal ligament cells via the heme oxygenase-1 pathway. *Int J Mol Med*. 2017;40(5):1591–1601. doi:10.3892/ijmm.2017.3129
36. Li J, Song L, Hou M, et al. Carbon monoxide releasing molecule-3 promotes the osteogenic differentiation of rat bone marrow mesenchymal stem cells by releasing carbon monoxide. *Int J Mol Med*. 2018;41(4):2297–2305. doi:10.3892/ijmm.2018.3437
37. American Diabetes Association. Classification and diagnosis of diabetes: standards of medical care in diabetes-2020. *Diabetes Care*. 2020;43(Suppl 1):S14–S31. doi:10.2337/dc20-S002

38. Ravi R, Balasubramaniam V, Kuppusamy G, et al. Current concepts and clinical importance of glycemic variability. *Diabetes Metab Syndr*. 2021;15 (2):627–636. doi:10.1016/j.dsx.2021.03.004
39. Kim HS, Park JW, Yeo SI, et al. Effects of high glucose on cellular activity of periodontal ligament cells in vitro. *Diabet Res Clin Pract*. 2006;74 (1):41–47. doi:10.1016/j.diabres.2006.03.034
40. Fu YW, He HB. Apoptosis of periodontium cells in streptozototocin- and ligature-induced experimental diabetic periodontitis in rats. *Acta Odontol Scand*. 2013;71(5):1206–1215. doi:10.3109/00016357.2012.757638
41. Liu J, Jiang Y, Mao J, et al. High levels of glucose induces a dose-dependent apoptosis in human periodontal ligament fibroblasts by activating caspase-3 signaling pathway. *Appl Biochem Biotechnol*. 2013;170(6):1458–1471. doi:10.1007/s12010-013-0287-y
42. Polak D, Shapira L. An update on the evidence for pathogenic mechanisms that may link periodontitis and diabetes. *J Clin Periodontol*. 2018;45 (2):150–166. PMID: 29280184. doi:10.1111/jcpe.12803
43. Sanz M, Ceriello A, Buysschaert M, et al. Scientific evidence on the links between periodontal diseases and diabetes: consensus report and guidelines of the joint workshop on periodontal diseases and diabetes by the International Diabetes Federation and the European Federation of Periodontology. *J Clin Periodontol*. 2018;45(2):138–149. PMID: 29280174. doi:10.1111/jcpe.12808
44. Kohmoto J, Nakao A, Kaizu T, et al. Low-dose carbon monoxide inhalation prevents ischemia/reperfusion injury of transplanted rat lung grafts. *Surgery*. 2006;140(2):179–185. doi:10.1016/j.surg.2006.03.004
45. Motterlini R. Carbon monoxide-releasing molecules (CO-RMs): vasodilatory, anti-ischaemic and anti-inflammatory activities. *Biochem Soc Trans*. 2007;35(Pt 5):1142–1146. doi:10.1042/BST0351142
46. Musameh MD, Fuller BJ, Mann BE, et al. Positive inotropic effects of carbon monoxide-releasing molecules (CO-RMs) in the isolated perfused rat heart. *Br J Pharmacol*. 2006;149(8):1104–1112. doi:10.1038/sj.bjp.0706939
47. Wei L, Hou M, Wang P, et al. Effect of carbon monoxide releasing molecule on experimental periodontitis in rats. *Hua Xi Kou Qiang Yi Xue Za Zhi*. 2014;32(1):23–26. doi:10.7518/hxkq.2014.01.006
48. Blufstein A, Behm C, Nguyen PQ, et al. Human periodontal ligament cells exhibit no endotoxin tolerance upon stimulation with Porphyromonas gingivalis lipopolysaccharide. *J Periodontal Res*. 2018;53(4):589–597. doi:10.1111/jre.12549
49. Darveau RP, Pham T-T-T, Lemley K, et al. Porphyromonas gingivalis lipopolysaccharide contains multiple lipid A species that functionally interact with both toll-like receptors 2 and 4. *Infect Immun*. 2004;72(9):5041–5051. doi:10.1128/IAI.72.9.5041-5051.2004
50. Herath TD, Darveau RP, Seneviratne CJ, et al. Tetra- and penta-acylated lipid A structures of Porphyromonas gingivalis LPS differentially activate TLR4-mediated NF-κB signal transduction cascade and immuno-inflammatory response in human gingival fibroblasts. *PLoS One*. 2013;8(3): e58496. doi:10.1371/journal.pone.0058496
51. Wang L, Wu J, Guo X, Huang X, Huang Q. RAGE plays a role in LPS-induced NF-κB activation and endothelial hyperpermeability. *Sensors*. 2017;17(4):722. PMID: 28358333; PMCID: PMC5421682. doi:10.3390/s17040722
52. Chen J, Peng H, Chen C, et al. NAG-1/GDF15 inhibits diabetic nephropathy via inhibiting AGE/RAGE-mediated inflammation signaling pathways in C57BL/6 mice and HK-2 cells. *Life Sci*. 2022;311(Pt A):121142. PMID: 36367498. doi:10.1016/j.lfs.2022.121142
53. Mollace A, Coluccio ML, Donato G, Mollace V, Malara N. Cross-talks in colon cancer between RAGE/AGEs axis and inflammation/immunotherapy. *Oncotarget*. 2021;12(13):1281–1295. PMID: 34194625; PMCID: PMC8238251. doi:10.18632/oncotarget.27990
54. Plemmenos G, Piperi C. Pathogenic molecular mechanisms in periodontitis and peri-implantitis: role of advanced glycation end products. *Life*. 2022;12(2):218. PMID: 35207505; PMCID: PMC8874682. doi:10.3390/life12020218
55. Sethi JM, Otterbein LE, Choi AM. Differential modulation by exogenous carbon monoxide of TNF-alpha stimulated mitogen-activated protein kinases in rat pulmonary artery endothelial cells. *Antioxid Redox Signal*. 2002;4(2):241–248. doi:10.1089/152308602753666299
56. Zhang X, Shan P, Otterbein LE, et al. Carbon monoxide inhibition of apoptosis during ischemia-reperfusion lung injury is dependent on the p38 mitogen-activated protein kinase pathway and involves caspase 3. *J Biol Chem*. 2003;278(2):1248–1258. doi:10.1074/jbc.M208419200
57. Indyk D, Bronowicka-Szydełko A, Gamian A, Kuzan A. Advanced glycation end products and their receptors in serum of patients with type 2 diabetes. *Sci Rep*. 2021;11(1):13264. PMID: 34168187; PMCID: PMC8225908. doi:10.1038/s41598-021-92630-0